

Synthesizing Sentiment-Controlled Feedback For Multimodal Text and Image Data

PUNEET KUMAR*, Center for Machine Vision and Signal Analysis, University of Oulu, Finland

SARTHAK MALIK*, Indian Institute of Technology Roorkee, India

BALASUBRAMANIAN RAMAN, Indian Institute of Technology Roorkee, India

XIAOBAI LI†, State Key Laboratory of Blockchain and Data Security, Zhejiang University, China

The ability to generate sentiment-controlled feedback in response to multimodal inputs comprising text and images addresses a critical gap in human-computer interaction. This capability allows systems to provide empathetic, accurate, and engaging responses, with useful applications in education, healthcare, marketing, and customer service. To this end, we have constructed a large-scale Controllable Multimodal Feedback Synthesis (CMFeed) dataset and propose a controllable feedback synthesis system. The system features an encoder, decoder, and controllability block for textual and visual inputs. It extracts features using a transformer and Faster R-CNN networks, combining them to generate feedback. The CMFeed dataset includes images, texts, reactions to the posts, human comments with relevance scores, and reactions to these comments. These reactions train the model to produce feedback with specified sentiments, achieving a sentiment classification accuracy of 77.23%, which is 18.82% higher than the accuracy without controllability. The system also incorporates a similarity module for assessing feedback relevance through rank-based metrics and an interpretability technique to analyze the contributions of textual and visual features during feedback generation. Access to the CMFeed dataset and the system's code is available at github.com/MIntelligence-Group/CMFeed.

CCS Concepts: • **Computing methodologies** → **Natural language generation**; *Machine learning*; • **Information systems** → **Sentiment analysis**; *Multimedia and multimodal retrieval*; • **Human-centered computing**;

Additional Key Words and Phrases: Affective Computing, Controllability, Interpretability, Multimodal Analysis.

ACM Reference Format:

Puneet Kumar, Sarthak Malik, Balasubramanian Raman, and Xiaobai Li. 2024. Synthesizing Sentiment-Controlled Feedback For Multimodal Text and Image Data. *ACM Trans. Multimedia Comput. Commun. Appl.* 1, 1, Article 1 (October 2024), 23 pages. <https://doi.org/XXXXXXXX.XXXXXXX>

1 INTRODUCTION

The process of multimodal feedback synthesis involves generating responses to multimodal inputs in a way that mimics human spontaneous reaction [35]. Controlling sentiments in feedback, a capability inherent to humans, remains a challenge for machines [43]. The ability to control sentiments in feedback synthesis facilitates more empathetic responses in healthcare, accurate marketing insights,

*Both authors contributed equally to this work

†Corresponding author

Authors' addresses: [Puneet Kumar](mailto:puneet.kumar@oulu.fi), puneet.kumar@oulu.fi, Center for Machine Vision and Signal Analysis, University of Oulu, Finland; [Sarthak Malik](mailto:sarthak_m@mt.iitr.ac.in), sarthak_m@mt.iitr.ac.in, Indian Institute of Technology Roorkee, India; [Balasubramanian Raman](mailto:bala@cs.iitr.ac.in), bala@cs.iitr.ac.in, Indian Institute of Technology Roorkee, India; [Xiaobai Li](mailto:xiaobai.li@zju.edu.cn), xiaobai.li@zju.edu.cn, State Key Laboratory of Blockchain and Data Security, Zhejiang University, China.

Permission to make digital or hard copies of all or part of this work for personal or classroom use is granted without fee provided that copies are not made or distributed for profit or commercial advantage and that copies bear this notice and the full citation on the first page. Copyrights for components of this work owned by others than ACM must be honored. Abstracting with credit is permitted. To copy otherwise, or republish, to post on servers or to redistribute to lists, requires prior specific permission and/or a fee. Request permissions from permissions@acm.org.

© 2024 Association for Computing Machinery.

1551-6857/2024/10-ART1 \$15.00

<https://doi.org/XXXXXXXX.XXXXXXX>

and engaging educational content while enabling systems to predict patients' mental states, assess product responses, analyze social behaviors, and gauge user engagement in advertisements [5, 22]. The controllability of these systems allows them to be customized for individual users, enhancing personalization [47].

The need for the Controllable Multimodal Feedback Synthesis (CMFeed) dataset arises from the requirement of a dataset containing human-generated feedback in addition to multimodal inputs. The CMFeed dataset has been created by crawling Facebook news articles and includes input images, texts, human comments, comments' metadata (such as likes, shares, reactions, and relevance scores), and sentiment labels. Unlike traditional sentiment-controlled text generation systems that do not utilize human comments, systems developed using the CMFeed dataset can be distinctively trained on human-generated comments to learn human-like spontaneity and contextual diversity. This enables the generation of 'opinions' rather than just 'knowledge' or 'facts,' which the proposed task focuses on. Our approach uniquely allows for the generation of controlled opinions.

Based on the CMFeed dataset, a novel task of controllable feedback synthesis for input images and text has been defined, and a feedback synthesis system has been proposed to generate sentiment-controlled feedback. It includes two networks for textual and visual modalities, each with an encoder, a decoder, and a control layer. The encoders use a text transformer [69] and a Faster R-CNN model [56] to extract features, which the decoder then combines for feedback generation. The control layer, positioned after the decoder, selectively activates or deactivates neurons to align with positive or negative sentiments as required. The system also incorporates a similarity module to ensure feedback aligns with the input context. To establish benchmarks for this new task, we compared our system against several baselines using different fusion methods and encoding strategies. The proposed system achieved a sentiment classification accuracy of 77.23%, significantly higher than the baselines. The major contributions of this paper are summarized as follows:

- A new dataset, CMFeed, has been constructed containing text, images, corresponding comments, number of likes, shares, and sentiment class. This dataset facilitates training multimodal feedback synthesis models to generate sentiment-controlled feedback for input containing images and text.
- A feedback synthesis system capable of generating sentiment-controlled feedback has been developed. It extracts textual and visual features using transformer and Faster R-CNN models and combines them to generate feedback.
- An interpretability technique, K-Average Additive exPlanation (KAAP) has been incorporated that analyzes the contributions of textual and visual features during feedback generation.
- A novel controllability module has been introduced, enabling sentiment regulation in the generated feedback. It selectively activates or deactivates neurons to ensure alignment of the feedback with the desired sentiment.

The remainder of the paper is organized as follows: the existing related works are surveyed in Section 2. Section 3 describes the dataset construction process and the proposed system. The experiments and results have been discussed in Section 4 and Section 4.4 respectively, and Section 5 outlines the discussions, conclusions and future directions.

2 RELATED WORKS

This section explores the related works to the proposed task of controllable feedback synthesis, including multimodal summarization, visual question answering, dialogue generation, and sentiment-aware text generation.

2.1 Multimodal Summarization

Multimodal summarization combines the inputs from various modalities to produce comprehensive summaries [91]. In this direction, Chen and Zhuge [12] used recurrent networks to align text with

corresponding images. In another work, Zhu et al. [89] focused on extractive summarization, selecting relevant images and texts using a pointer generator network. Their work was extended by Zellers et al. [84] for video summarization, using self-attention mechanisms to choose relevant video frames based on semantic content. Shang et al. [64] emphasized timing in video summarization with time-aware transformers. In other studies, Zhao et al. [85] explored audiovisual video summarization including sensory input and Xie et al. [79] used visual aesthetics while generating multimodal summaries.

Despite the advancements mentioned above, multimodal summarization faces the challenge of modality bias [51, 90], and it has not been explored for affect synthesis. Moreover, multimodal summarization approaches do not incorporate human comments in their model training. In contrast, the proposed system is trained on human-generated comments alongside text and image inputs to generate sentiment-controlled feedback. Furthermore, unlike multimodal summarization, which condenses the given information, controllable feedback synthesis produces feedback that aligns with sentiments and fits the context.

2.2 Visual Question Answering

Visual Question Answering (VQA) combines visual perception with interactive question answering [3]. Chen et al. [11] explored controlled generation versus standard answering methods in VQA, while Wang et al. [72] focused on fact-based control to improve response accuracy. Cascante et al. [8] introduced an innovative approach using synthetic data, including 3D and physics simulations, to expand VQA's scope and enhance model adaptability. Furthermore, Jin et al. [30] proposed a text-based VQA system that explored the correlation between the text in the images and the visual scene. In another work, Guo et al. [24] developed a universal quaternion hypergraph network for advanced multimodal video question answering.

Contributions like Wu et al.'s [76] memory-aware control in community question answering and Lehmann et al.'s [38] use of language models for knowledge graph question answering illustrate VQA's diverse applications. Furthermore, Ishmam et al. [28] discuss the contemporary shift towards vision language pre-training techniques and highlight the challenges in integrating traditional VQA approaches with modern VLP methods. The developments in VQA, however, stand in contrast to the proposed task of sentiment-controlled feedback synthesis. While VQA focuses on generating accurate responses to questions, sentiment-controlled feedback synthesis is centered on creating responses to multimodal stimuli (images and text) that are contextually relevant.

2.3 Dialogue Generation

In dialogue generation, particularly in visual dialogue (VisDial), computational models are designed to engage in dialogues about the visual content present in images. In this direction, Kang et al. [32] developed a dual Attention Network that utilized the understanding of visual references in dialogues. This approach was further advanced by Jiang et al. [29], who implemented a region-based graph attention network for enhanced image-related questioning. In other works, Xu et al. [81] and Zhao et al. [86] worked on modeling the conversations utilizing conditional variational autoencoders for diverse dialogue scenarios.

Recent developments in VisDial include the work of Chen et al. [10], who applied contrastive learning for better cross-modal comprehension in visual dialogue. Contributions from Wang et al. [73] and Kang et al. [31] involved enhanced dialogue generation through generative self-training. Liu et al. [41] and Liu et al. [40] also contributed to closed-loop reasoning and counterfactual visual dialogue for unbiased knowledge training. Despite the aforementioned developments, existing VisDial methods do not generate sentiment-controlled feedback. The proposed system stands apart as it synthesizes feedback that is not only contextually relevant but is also tailored to the sentiment of the conversation.

2.4 Sentiment-Aware Conversation Agents

In the context of sentiment-aware conversational agents, Das et al. [14] laid the groundwork by using multiple generators and a multi-class discriminator to create text with diverse sentiment tones. Building upon this, Shi et al. [66] introduced a framework leveraging user sentiments to guide dialogue actions. In another work, Kong et al. [33] explored sentiment-constrained dialogue generation using generative adversarial networks. In recent developments, Firdaus et al. [20] presented a system that integrates sentiments into conversational agents. Their SEPRG model complemented it [21], which focuses on sentiment-aware, sentiment-controlled personalized response generation. In other works, Hu et al. [25] developed a speech sentiment-aware agent for empathetic responses, and Saha et al. [61] integrated sentiment-aware mechanisms into conversation generation. Unlike the aforementioned works that primarily focus on recognizing the users' sentiments and using the same to influence dialogue actions, the proposed system generates (as opposed to recognizing) the feedbacks with the desired sentiment tone.

2.5 Sentiment-Controlled Text Generation

Recent natural text generation research trends include sentiment-controlled text generation. In this context, Zhou et al. [88] introduced the emotional chatting machine, employing a seq2seq framework with internal and external memories for managing emotional states. In another work, Wang and Wan [71] generated sentimental texts using mixture adversarial networks. Huang et al. [26] contributed to automatic dialogue generation with a focus on expressed emotions. Building on these, Zhong et al. [87] introduced an affective attention mechanism with a weighted cross-entropy loss for generating affective dialogue. Extending the scope of sentiment control into other domains, Wu et al. [77] developed Music ControlNet, a diffusion-based model that manipulates time-varying controls such as melody, rhythm, and dynamics in music generation, paralleling the challenges in sentiment-controlled text generation. Similarly, Yang et al. [82] enhanced text-to-image models by employing glyph information to precisely control text placement and size in images, demonstrating advanced customization capabilities in multimodal interactions.

The sentiment-controlled text generation methods do not use human comments to train their models. On the contrary, the proposed system captures the wider sentiment context from multimodal (text and images) inputs. Moreover, it is trained on human-generated comments aside from text and images to learn the contextual diversity from the comments. Furthermore, our work generates 'opinions' in contrast to generation of 'knowledge' or 'facts' by the above mentioned tasks. Unlike facts, the opinions can be controlled in a similar way how humans do. This area has not been addressed by the tasks mentioned earlier, while our work actively contributes towards it.

The datasets used for the aforementioned methods are summarized in Table 1. While a few include human-generated summaries or answers, none offer the metadata (such as relevance, reactions, and sentiment labels) necessary for training feedback synthesis systems. The absence of human comments and metadata in existing datasets hinders the development of sentiment-controlled feedback synthesis systems [35, 78]. In contrast, CMFeed addresses this gap by supporting the development of models that can generate opinions mimicking human conversational dynamics, a feature not covered by existing tasks. This capability enables CMFeed to create more personalized and contextually aware multimodal interactions, allowing sentiment to reflect the natural ebb and flow of human emotions. In contrast to the latest large language models (LLMs) such as Generative Pre-Trained Transformer (GPT) [53], which primarily excel in summarization and question answering through knowledge retrieval, the CMFeed dataset is designed to interpret multimodal inputs and produce novel, sentiment-controlled feedback that mimics human interaction, thereby marking a distinct contribution from conventional LLMs that rely on existing knowledge. Further, LLMs are prone to mistakes and

Table 1. Related datasets. ‘HC’: Human Comments, ‘CM’: Comments’ Metadata, ‘V’: Visual, ‘A’: Audio, ‘T’: Textual, ‘MMSum’: Multimodal Summarization, ‘VQA’: Vis Qu Ans, ‘VisDial’: Vis Dialogue, ‘SATextGen’: Sentiment-Aware Text Generation, ‘N/A’: Not Applicable, ‘-’: Unavailable.

| Area | Dataset | Year | Dataset Size | No. of Subjects | Modalities | HC | CM |
|-----------|---------------------|------|-----------------------|-------------------|------------|----|----|
| MMSum | VMSMO [84] | 2020 | 184920 documents | 70 participants | V, T | ✓ | ✗ |
| | MMSMO [89] | 2018 | 314581 documents | 10 students | V, T | ✓ | ✗ |
| | MVSA-Single [48] | 2016 | 4869 tweets | N/A | V, T | ✗ | ✗ |
| | MVSA-Multiple [48] | 2016 | 4869 tweets | N/A | V, T | ✗ | ✗ |
| VQA | DocVQA [45] | 2020 | 50K QA pairs | - | T | ✗ | ✗ |
| | OK VQA [44] | 2019 | 150K QA pairs | 5 MTurk workers | V, T | ✗ | ✗ |
| | VQA [23] | 2017 | 1.1M QA pairs | 215 MTurk workers | V, T | ✓ | ✗ |
| | VideoQA [80] | 2017 | 243K QA pairs | - | V, T | ✗ | ✗ |
| VisDial | InfoVisDial [74] | 2023 | 79535 dialogues | 35 annotators | V, T | ✗ | ✗ |
| | CLEVR-Dialog [34] | 2019 | 4.25M dialogues | - | V, T | ✗ | ✗ |
| | VisDial [15] | 2017 | 1.23M QA pairs | 200 annotators | V, T | ✓ | ✗ |
| | Visual Madlibs [83] | 2015 | 397675 dialogues | 1 quality checker | V, T | ✗ | ✗ |
| SATextGen | SEPRG [21] | 2021 | 64356 conversations | 500 samplers | T | ✓ | ✗ |
| | EMOTyDA [60] | 2020 | 19365 videos | 10 participants | V, T | ✓ | ✗ |
| | ESTC [88] | 2018 | 4308211 conversations | - | T | ✓ | ✗ |
| | STC [63] | 2015 | 4.4M conversations | - | T | ✓ | ✗ |

hallucinations [19, 27]. They are auto-regressive and black-box. Autoregressive means if the first few words are wrong, it may lead to incorrect generation of subsequent words. The internal mechanisms, such as which modality influences the response, are generally not transparent. By incorporating the proposed interpretability mechanism detailed in Sections 3.3.7 and 4.4.5, we have demonstrated how metadata and multimodal features influence responses and how sentiments are learned. In fact, the proposed concepts of controllability and interpretability can inspire new ideas for the LLMs and other related tasks such as VisDial.

3 PROPOSED METHODOLOGY

3.1 Dataset Construction

3.1.1 Data collection. The CMFeed dataset has been compiled by crawling news articles from Sky News, NYDaily, FoxNews, and BBC News through Facebook posts. The data collection process utilized the NLTK [4] & newspaper3k [50] libraries and it was conducted in compliance with Facebook’s terms and conditions [46], ensuring adherence to all legal and ethical standards.

Choice of Facebook for Dataset Construction: Facebook was chosen for data collection due to its unique provision of metadata such as news article links, post shares, post reactions, comment likes, comment rank, comment reaction rank, and relevance scores, which are not available on other platforms. With 3.07 billion monthly users, it is the most used social media platform, compared to Twitter’s 550 million and Reddit’s 500 million [75]. Broad popularity is maintained across various age groups, with at least 58% usage among ages 18-29, 30-49, 50-64, and above 65, significantly surpassing the 6% for Twitter and 3% for Reddit [67]. This trend is consistent across demographics such as gender, race, ethnicity, income, education, community, and political affiliation [9]. The male-to-female user ratio is reported as 56.3% to 43.7% on Facebook, compared to Twitter’s 66.72% to 23.28%; such data are not reported by Reddit [17]. These characteristics make Facebook an ideal platform for the collection of a diverse and representative dataset.

Choice of News Handles: Four news handles—BBC News, Sky News, Fox News, and NY Daily News—were selected to ensure diversity and comprehensive regional coverage. These news outlets were chosen for their distinct editorial perspectives and regional focuses: global coverage and centrist views are known from BBC News, targeted content and center/right leanings in the UK, EU, and US are offered by Sky News, right-leaning content in the US is recognized from Fox News, and left-leaning coverage in New York is provided by NY Daily News. A broad spectrum of political discourse and audience engagement is ensured by this selection.

3.1.2 Preprocessing. The CMFeed dataset consists of multiple images per sample, corresponding news text, post likes and shares, and human comments along with reactions and shares. The comments for each post have been sorted based on Facebook’s ‘most-relevant’ criterion, which prioritizes the comments with the highest likes and shares. The comments have been preprocessed as follows: emoticons converted to words using the Demoji library [68]; blank comments removed; contractions expanded; special and accented characters eliminated; punctuations and numbers purged to reduce noise; stop-words removed; and comments converted to lowercase. These steps are designed to reduce noise while retaining key sentiment cues in the text. This approach is based on the understanding that core sentiments are primarily conveyed through words, not punctuation or numbers. As per Facebook’s ethical protocols, we used manual data scraping and strategically chose 1000 posts from each of four news handles—BBC News, Sky News, Fox News, and NY Daily News—to promote diversity and reduce bias. Initially, 4000 posts were collected; however, after preprocessing, 3646 posts remained. Subsequently, all associated comments were processed, yielding a total of 61734 comments. As summarized in Table 2, on average, each news post received 65.1 likes, while comments averaged 10.5 likes. The average length of news text was 655 words. Additionally, each post contained an average of 3.7 images.





Table 2. CMFeed dataset’s overview.

| Parameter | Value |
|--------------------------------|-----------|
| No. of news posts | 3646 |
| No. of total data samples | 61734 |
| No. of samples after filtering | 57222 |
| Avg. no. of likes per post | 65.1 |
| Avg. no. of likes per comment | 10.5 |
| Avg. length of news text | 655 words |
| Avg. no. of images per post | 3.7 |

3.1.3 Annotation Strategy. : To determine the ground-truth sentiment labels for the comments, we obtained sentiment scores using four pre-trained models: FLAIR Library [1], SentimentR [57], DistilBERT [62], and RoBERTa [42]. Each of these models has unique capabilities: FLAIR specializes in capturing contextual variations in text using a neural network approach. SentimentR is designed to analyze textual sentiments by evaluating linguistic cues within the text. DistilBERT and RoBERTa are both transformer-based models optimized for understanding the nuances of language through self-attention mechanisms. DistilBERT offers a lighter, faster variant of BERT that retains most of its predictive power, whereas RoBERTa is trained on an even larger corpus with more robust fine-tuning, enhancing its ability to discern complex sentiment patterns.

We adopted a majority voting strategy for annotation, similar to that used in the construction of the IEMOCAP dataset [7], retaining data samples that received the same sentiment class from at least three of the four models. The remaining samples were excluded and marked with the sentiment class ‘XX.’ The models generated sentiment values of -1 or 1 along with a confidence score. We

Table 3. Representative samples from the CMFeed dataset. Here, ‘PLikes’ (Post Likes) and ‘CLikes’ (Comment Likes) show the number of likes for the post and comment, respectively; ‘Shares’ denotes number of shares for the post and ‘C’ represents comment’s sentiment class (1: positive, 0: negative).

| Title | Text | Images | PLikes | Shares | Comment | CLikes | C |
|---|---|--|--------|--------|--|--------|---|
| There are costs of managing beavers, but the benefits outweigh those costs. | Beaver dams in east Devon create area of wetland amid drought. The dams have created a wetland despite the dry weather. A network of dams built by beavers in Devon has helped to maintain an area of wetland despite a drought in the South West. There are a number of beavers ... |  | 2887 | 165 | Benefits outweigh the costs because beavers are ecosystem engineers! | 47 | 1 |
| A national emergency has been declared. | Pakistan floods: Monsoons bring misery to millions in Pakistan By Pumza Fihlani in Sukkur, Pakistan and Frances Mao in Singapore. Millions of people have been affected by floods in Pakistan, hundreds have been killed, and the government has declared a national emergency ... |  | 2005 | 126 | Circumstances are really miserable after monster floodings. | 26 | 0 |
| Celebrating his birthday, John Tinniswood said moderation in everything. | Moderation is the key to life, GB’s oldest man says on 110th birthday, Mr Tinniswood was joined by family and friends to celebrate his big day. Britain’s oldest man has celebrated his 110th birthday by declaring “moderation in everything and all things” as the secret ... |  | 12000 | 407 | Congratulations on a well lived life and 110. | 31 | 1 |
| If it leaks then it’s easy to clean. | Bin strikes: The people using baths and hiring skips to store rubbish, Helen Sikora has been keeping rubbish bags in her bath so she can easily clean up any leaks. Edinburgh residents have told how they have hired skips and used bathtubs to store rubbish, as waste piles up ... |  | 464 | 29 | Dump it on streets if they do not bother to collect it. | 29 | 0 |

calculated a score by multiplying the sentiment value by its confidence, then normalized this score to a range between 0 (negative sentiment) and 1 (positive sentiment). Averages of these normalized scores across the models provided the final sentiment labels. To further ensure robustness, we also employed a safety margin from 0.49 and 0.51 and marked the labels with the score in this range as ‘XX.’ Of the total 61734 samples analyzed, 57222 met the criteria for inclusion in further experiments based on the above filtering strategies, ensuring high confidence in the ground-truth labels.

The sentiment prediction was conducted on comments to capture and analyze direct human emotional reactions, independent of the original text or imagery. This approach aims to understand user reactions, which are direct, spontaneous, and personal, thus providing insights into user sentiments. The objective is to enable the feedback synthesis system to emulate this human-like directness and spontaneity. To ensure the accuracy of the constructed ground-truth sentiment labels, a human evaluation was conducted. 50 evaluators (25 males and 25 females, average age 30 ± 2.73 years) assessed the sentiment of 50 randomly selected pairs of input image and text. The results showed that 90.88% of evaluators (standard deviation 7.59%) agreed on the consistency between the expressed sentiment and the assigned sentiment label.

The CMFeed dataset’s sample instances have been depicted in Table 3. Multiple images and comments correspond to each news post, enabling the feedback synthesis model to learn the comments’ contextual diversity and relevance with the input. The CMFeed dataset can be accessed at zenodo.org/records/11409612 along with detailed description of its metadata, collection process, intended

usage, licensing, and handling. The corresponding code can be accessed at github.com/MIntelligence-Group/CMFeed/.

3.2 Task Formulation

Given an environment $E = \{T, I_1, I_2, \dots, I_n\}$, where T denotes input text and I_1, I_2, \dots, I_n denote n input images. Each image is comprised of m objects o_1, o_2, \dots, o_m , while the text T is made up of a dictionary of k words w_1, w_2, \dots, w_k . The task is to generate a feedback towards environment E under a sentiment-controlled manner where ‘sentiment-controlled’ implies the feedback aligns with a specified sentiment S , with S being either 0 for a negative sentiment or 1 for a positive sentiment.

3.3 Proposed Feedback Synthesis System

The proposed system, as illustrated in Fig. 1, includes two networks for processing textual and visual data, each with an encoder, a decoder, and a control layer. It extracts textual and visual features using a text transformer [69] and a Faster R-CNN model [56], respectively. These features are then used by the decoders to generate feedback. The system also includes a similarity module to evaluate the feedback’s contextual alignment with human comments. From input images and text, the proposed system uses encoders to extract features, integrating visual and textual information to comprehend the content and its context thoroughly. It also learns from comments to analyze sentiment and user engagement, which helps in crafting responses that mirror human emotional reactions. Overall, the system synthesizes these insights to generate sentiment-controlled feedback that is contextually relevant and emotionally resonant, adapting its output to match the desired sentiment.

3.3.1 Textual Encoder. The textual encoder utilizes a transformer model [69], featuring global encoding and textual attention mechanisms. Global encoding is enhanced by a convolution-gated unit to improve textual representation, reduce repetition, and maintain semantic relevance. The textual attention component includes multi-headed self-attention, comprising a self-attention layer and a feed-forward layer. Positional embedding captures token positioning, and normalization finalizes the process to produce the textual context vector z_i^* . The feed-forward network (FFN) includes input and output layers with a dimension of 512 and a hidden layer of 2048. The FFN’s output for a specific input x is defined in Eq. 1.

$$FFN(x) = \max(0, xW_1 + b_1)W_2 + b_2 \quad (1)$$

where, b_1 , b_2 , W_1 , and W_2 represent the bias terms and weight matrices, respectively. In the self-attention mechanism, the query, key, and value weight matrices are initially randomized in the encoder and updated during training.

3.3.2 Visual Encoder. The top three images from each sample are inputted into a visual encoder, using blank images when fewer are available. Features extracted from these images are concatenated to form a visual context vector z_i^* . This process employs a pre-trained Faster R-CNN model [56]. According to Eq. 2, CNN layers produce feature maps that the Region Proposal Network (RPN) uses to create anchor boxes with binary scores based on Intersection Over Union (IoU) values [58]. These anchors are then classified and regressed to yield classified boxes. A total of 1601 classes are assigned to these boxes, and their features are combined into a global feature vector. Faster R-CNN is selected for its efficiency and precision in detecting small and varied objects, suitable for non-real-time settings. The choice to use the top three images strikes a balance between retaining essential visual content and minimizing blank images in posts with fewer images, considering most posts have at least three images.

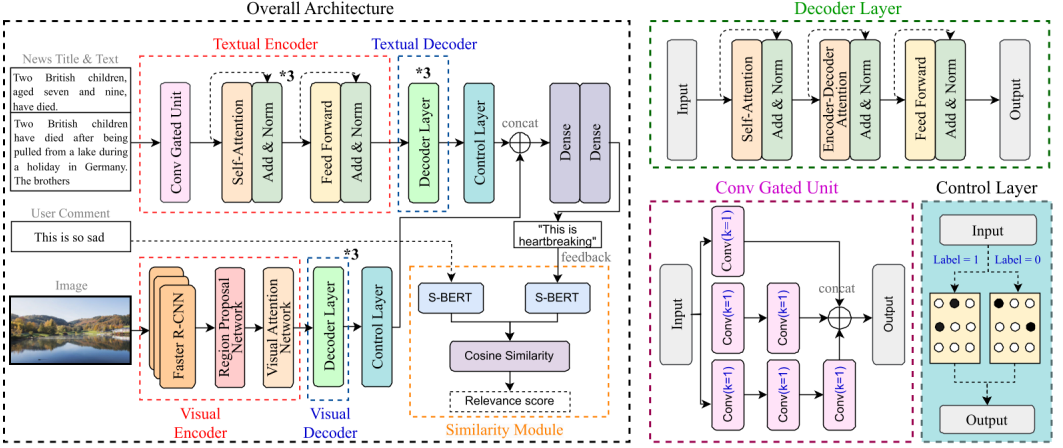


Fig. 1. Proposed feedback synthesis system's architecture with encoder, decoder, and controllability blocks for textual and visual data. The decoder, convolution-gated unit, control layer, and similarity modules are shown as distinct subblocks while off & on neurons are shown as black & white circles.

$$Objectiveness\ Score = \begin{cases} Positive; & IoU > 0.7 \\ Negative; & IoU < 0.3 \\ No\ score; & 0.3 < IoU < 0.7 \end{cases} \quad (2)$$

3.3.3 Attention. The attention mechanism in both the encoder and decoder operates on three vectors: Q (query), K (key), and V (value). The output of the self-attention layer, denoted as z_i , is computed by multiplying the i^{th} input vector of the encoder with the respective weight matrices $W(Q)$, $W(K)$, and $W(V)$. This computation yields the attention head matrix z , as detailed in Eq. 3, whose dimensionality is equivalent to the length of the input sequence.

$$z = Attention(Q, K, V) = softmax\left(\frac{Q \cdot K^T}{\sqrt{d_k}}\right)V \quad (3)$$

where Q , K , and V represent matrices that contain all queries, keys, and values, respectively, with d_k as the scaling factor and K^T denoting the transpose of K . To achieve a comprehensive subspace representation, the mechanism computes multiple attention heads using distinct sets of Query, Key, and Value matrices. The queries, keys, and values undergo projection $head$ times, resulting in multiple attention heads $h_1, h_2, \dots, h_{head}$, where $head$ signifies the total number of heads. These heads are then concatenated and multiplied by the weight matrix W , producing the intermediate output vector z' , as delineated in Eq. 4.

$$\begin{aligned} h_i &= Attention(QW^Q_i, KW^K_i, VW^V_i) \\ z' &= Concat(h_1, h_2, \dots, h_{head})W^O \end{aligned} \quad (4)$$

where W^Q_i , W^K_i , W^V_i , and W^O_i are the respective projections of queries, keys, values, and output of corresponding heads. The final context vector z^* is then derived by passing this intermediate output through the feed-forward layer.

3.3.4 Decoder. The textual and visual decoders share a similar structure, each consisting of two main blocks: a self-attention block and an encoder-decoder attention block, enhanced with positional

encoding and normalization for improved efficiency and accuracy. The textual decoder processes the textual context vector z_t , while the visual decoder handles the visual context vector z_i . Both decoders also receive the ground-truth comment as input. The self-attention layer uses future position masking to focus only on previous positions in the output sequence, with its weight matrices initially random and refined during training. The encoder-decoder attention layer uses the context vectors z_t or z_i as keys and values, respectively. Late fusion is applied via concatenation to maintain distinct image feature information, and a gated convolution unit is incorporated for textual features to reduce repetition in the feedback.

3.3.5 Control Layer. The control layer, positioned after the decoder and before feedback generation, introduces perturbations to ensure feedback aligns with desired sentiments. It utilizes two masks, one each for positive and negative sentiments, altering the input vector via element-wise multiplication as per Eq. 5. This layer functions like a modified dropout layer, selectively activating or deactivating neurons to tune sentiment in the feedback, ensuring it matches the targeted tone.

$$O = \begin{cases} \text{mask}_1 * I; & \text{Sentiment} = 0 \\ \text{mask}_2 * I; & \text{Sentiment} = 1 \end{cases} \quad (5)$$

where O and I denote the output and input vectors, respectively. In this setup, each mask blocks $x\%$ of neurons, targeting different neuron sets. Consequently, $(100 - 2x)\%$ of neurons are trained on both sentiments, while $x\%$ are specialized for a specific sentiment, with $x\%$ set at 10%. This configuration helps direct the feedback towards the desired sentiment tone. During inference, to generate sentiment-specific feedback, neurons trained for the contrasting sentiment are deactivated. For instance, to produce positive feedback, neurons associated with negative sentiment are turned off, and vice versa. This method is crucial for controlling the output sentiment independently of the input text's sentiment, focusing on steering the generated sentence's sentiment.

3.3.6 Similarity Module. The similarity module quantitatively assesses the semantic similarity between the feedbacks generated by the proposed system and human comments, using a pre-trained Sentence-BERT (SBERT) model [55]. It transforms individual comments and feedbacks into vectors in an n -dimensional embedding space, where n is the size of the embeddings produced by the model. Each dimension represents a distinct linguistic feature or attribute, effectively capturing the sentence's semantic characteristics. After generating these embeddings, the cosine similarity between the vector representations of the generated feedback and the human-provided comment is computed. This cosine similarity score, a robust metric for this purpose, captures the orientation of the sentence vectors, reflecting their semantic similarity and providing a measure of relevance between the feedbacks and comments.

3.3.7 Interpretability. This section proposes an interpretability technique using the K-Average Additive exPlanation (KAAP) method [36] to analyze the contribution of textual and visual features towards feedback generation. It is based on Shapley Additive exPlanations (SHAP) that is an approximation of Shapley values [65]. As depicted in Fig. 2, it has been incorporated to assess the influence of each visual and textual feature on the sentiment portrayed by the generated feedback. We hypothesize that varying sentiments produced from identical inputs (text + images) should reflect in differential feature importance. It is expected that key features will differ for negative versus positive sentiments. When identical inputs are processed to portray varied sentiments, the model should adjust its focus across different image and text segments, thereby validating our controllability hypothesis.

SHAP Values Computation: The SHAP values for the features denote their contribution to the model's prediction. For a model f , the SHAP value for feature i is defined as per Eq. 6.

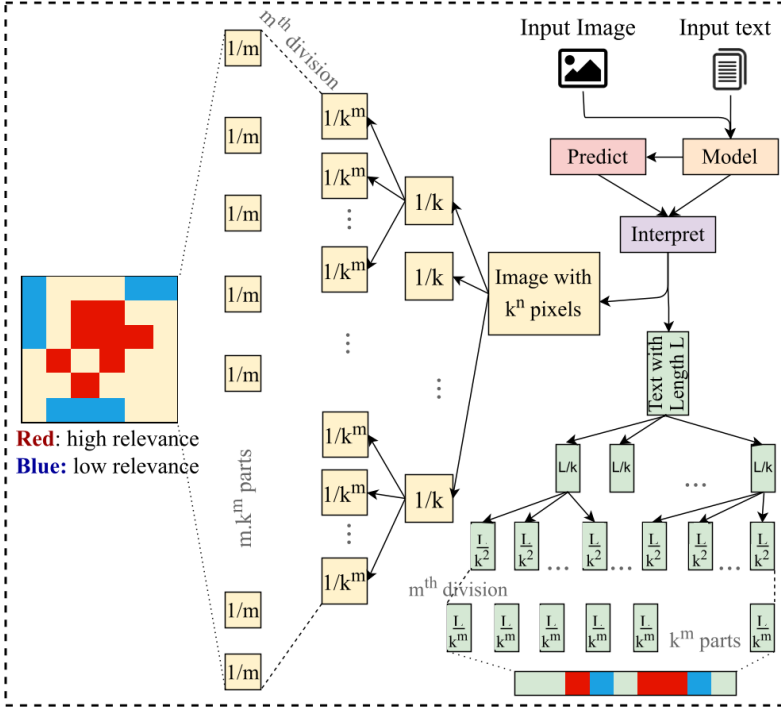


Fig. 2. Representation of the proposed interpretability technique. Here k_i and k_t denote the number of partitions for image and text, w_i is the image's width, and L_t is the text feature vector's length.

$$\mathcal{S}_i(f) = \sum_{S \subseteq F \setminus \{i\}} \frac{|S|!(|F| - |S| - 1)!}{|F|!} [f(S \cup \{i\}) - f(S)] \quad (6)$$

where F denotes the complete feature set, S a subset excluding i , and $f(S)$ the model's prediction using features in S .

The computation of SHAP values requires exponential time theoretically which is approximated by dividing the input into k parts as illustrated in Eq. 7. For each modality, the input is repeatedly divided into k segments, determining each segment's impact on model predictions. A feature vector X with n features is segmented into k parts.

$$X = [X_1, X_2, \dots, X_k], \text{ where } X_i \subseteq X \text{ and } \bigcup_{i=1}^k X_i = X \quad (7)$$

For simplicity with $k = 2$, the fundamental computation of SHAP values is denoted in Eq. 8. It is extended for other values of k . The optimal values of k_{img} and k_{txt} , representing the number of segments to divide the image and text into, have been determined experimentally.

$$\mathcal{S}_{\{f_1\}} + \mathcal{S}_{\{f_2\}} = \mathcal{S}_{\{f_1, f_2\}} - \mathcal{S}_{\{\text{null}\}} \quad (8)$$

K-Average Additive exPlanation (KAAP): The KAAP value for feature i is calculated by averaging the SHAP values across the k divisions of the feature vector using Eq. 9.

$$\text{KAAP}_i = \frac{1}{k} \sum_{j=1}^k \mathcal{S}_i(X_j) \quad (9)$$

The KAAP values directly indicate the significant image features for predictions. For input image X^{img} of dimensions 128×128 , the KAAP values for a given k are computed by segmenting the input along both axes. For text data X^{txt} , we derive the feature vector and divide it into k segments. Text division considers each word as a feature, acknowledging that sentiments are conveyed by words, not individual letters.

4 EXPERIMENTAL RESULTS

4.1 Training Strategy and Parameter Tuning

The proposed models have been trained for 60 epochs on an Nvidia V100 GPU, employing 5-fold cross-validation and an 80%-20% training-testing split.

- *General parameters* – Batch size: 16, learning rate: 0.001, network optimizer: Adam, loss function: cross-entropy loss, activation function: ReLU.
- *Parameters for the transformer model* – Encoder embedding dimensions: 100, decoder embedding dimensions: 100, encoder hidden units dimensions: 128, decoder hidden units dimensions: 128, encoder dropout: 0.1, decoder dropout: 0.1, encoder no. of layers and attention heads: 3 and 8, decoder no. of layers & attention heads: 3 and 8, metric: accuracy.
- *Parameters for the Faster R-CNN model* – No. of epochs: 18, no. of proposals: 18, no. of anchor-box classes: 1601, network optimizer: adaDelta, metric: mAP (mean Average Precision).

4.2 Evaluation Metrics

Feedback synthesis is a one-to-many task, i.e., many feedbacks can be generated for one pair of image-text input. Hence, computing the accuracy of generated feedbacks is not feasible. Instead, we evaluate the generated feedbacks against the ground-truth comments using the metrics to evaluate semantic relevance and their ranks. For semantic relevance evaluation, Bilingual Evaluation Understudy (BLEU) [52], Consensus-based Image Description Evaluation (CIDEr) [70], Recall-Oriented Understudy for Gisting Evaluation (ROUGE) [39], Semantic Propositional Image Captioning Evaluation (SPICE) [2], and Metric for Evaluation of Translation with Explicit ORdering (METEOR) [37] have been used. The BLEU is a precision-based metric, ROUGE is a recall-based metric, while METEOR combines precision and recall. On the other hand, CIDEr is a consensus-based evaluation metric, and SPICE is based on evaluating the sensitivity of n-grams. Higher values of these metrics denote more semantic similarity between the generated feedback and ground-truth comment. For ranking-based evaluation, we use ‘Mean Reciprocal Rank’ [13] and ‘Recall@k’ [59] defined below.

Mean Reciprocal Rank: For calculating the Mean Reciprocal Rank (MRR), first, the similarity of the generated feedback is compared with all the ground-truth comments. If the most similar comment is ranked k , then the rank of the j^{th} feedback is given by Eq. 10.

$$\text{rank}_j = k \quad (10)$$

where k denotes the k^{th} comment when sorted by the relevance whereas rank_j is the Rank of the j^{th} feedback. Finally, MRR is calculated as the average of the reciprocal ranks of all the generated feedback samples as per Eq. 11.

$$MRR = \left(\frac{1}{n}\right) \sum_{j=1}^n \frac{1}{rank_j} \quad (11)$$

where n is the number of generated feedback samples, while $rank_j$ denotes the j^{th} feedback's rank.

Recall@k: Recall@k counts the number of data samples matching any top- k relevant data samples. Adapting Recall@k to evaluate the generated feedback, the number of feedbacks similar to any of the top- k comments sorted according to relevance is calculated. To find if the generated feedback is similar to any comment, the rank of that feedback as calculated in Eq. 11 is used. Finally, the Recall@k can be formulated according to Eq. 12. According to this, if the rank of the feedback is in top- k , then a score of 1 is assigned to the feedback, else 0. The summation of all scores is done to calculate the Recall@k as shown in Eq. 12.

$$\begin{aligned} Recall@k_i &= 1 \text{ if } rank_i \in [1, \dots, k] \\ Recall@k &= \sum_{i=1}^n Recall@k_i \end{aligned} \quad (12)$$

where $Recall@k_i$ and $rank_i$ show i^{th} feedback's Recall@k and rank, respectively and $Recall@k$ is the final score. Furthermore, the sentiments of the generated feedbacks have been computed and sentiment classification accuracy has been analysed along with the 'Control Accuracy' which is the difference between the accuracies of controlled and uncontrolled feedbacks.

4.3 Models

The following constructed models have their architectures determined as per the ablation studies detailed in Section 4.4.7. Each includes the Controllability module outlined in Section 3.3.5, with the remaining architecture as follows.

- *Baseline 1* utilizes Gated Recurrent Units (GRU) as textual and VGG network as visual encoders. An early fusion method is applied to integrate visual and textual modalities.
- *Baseline 2* uses a late fusion approach for combining the visual and textual data while maintaining GRU for textual encoding and VGG for visual encoding.
- *Baseline 3* implements a combination of a Transformer and a gated convolutional unit for textual encoding. It uses Faster RCNN with an additional visual attention mechanism for visual encoding. A late fusion strategy with averaging is used here.
- *Baseline 4* replaces the textual encoder with GPT-2 [49] and continues to Faster RCNN for visual data encoding with visual attention. It also combines the modalities using a late fusion with averaging. It has been empirically observed that GPT-2 based model generated good feedbacks only for textual input; however, it did not generate good feedbacks for multimodal input.
- *Proposed System* incorporates Transformer as the textual encoder and Faster RCNN as the decoder and it uses concatenation along with late fusion.

4.4 Results

The results of the proposed benchmark feedback synthesis system are presented as follows.

4.4.1 Semantic Relevance Evaluation. The generated feedbacks' semantic relevance with human comments has been evaluated. The feedbacks are generated to reflect the same sentiment class as reflected by the corresponding comments and then the feedbacks are evaluated using the

BLEU, CIDEr, ROUGE, SPICE, and METEOR metrics. As depicted in Table 4, the proposed model has obtained the best values for these metrics in most cases.

Table 4. Semantic Relevance Evaluation.

| Model | BLEU | CIDEr | ROUGE | SPICE | METEOR |
|-------------------|---------------|---------------|---------------|---------------|---------------|
| Baseline 1 | 0.1942 | 0.1342 | 0.2527 | 0.1028 | 0.0929 |
| Baseline 2 | 0.2122 | 0.1635 | 0.2748 | 0.1654 | 0.1394 |
| Baseline 3 | 0.2093 | 0.1835 | 0.2377 | 0.1555 | 0.1407 |
| Baseline 4 | 0.1953 | 0.1798 | 0.2471 | 0.1478 | 0.1407 |
| Proposed | 0.3020 | 0.1817 | 0.3378 | 0.1554 | 0.1412 |

4.4.2 Rank-based Evaluation. The generated feedbacks are evaluated using MRR and Recall@k. As observed in Table 5, 76.58% feedbacks are relevant to one of the top 10 comments and the MRR of 0.3789 denotes that the generated feedbacks are contextually similar to one of the top 3 comments.

Table 5. Rank-based Evaluation. Here, ‘MMR’ and ‘R@k’ denote ‘Mean Reciprocal Rank’ and ‘Recall@k’ where $k \in \{1,3,5,10\}$.

| Model | MRR | R@1 | R@3 | R@5 | R@10 |
|-------------------|---------------|--------------|--------------|--------------|--------------|
| Baseline 1 | 0.3435 | 17.30 | 39.67 | 60.67 | 67.75 |
| Baseline 2 | 0.3305 | 17.69 | 36.99 | 61.47 | 74.29 |
| Baseline 3 | 0.3214 | 16.08 | 37.53 | 59.32 | 69.29 |
| Baseline 4 | 0.3182 | 16.98 | 37.26 | 56.11 | 71.29 |
| Proposed | 0.3789 | 18.76 | 40.92 | 60.13 | 76.58 |

The variations in sentiment classification accuracy and MRR varied differently for different models. For example, baseline 4 has lower MRR but high sentiment classification accuracy, whereas it is reverse for baseline 3. The proposed model provides the right trade-off with high values for both.

4.4.3 Sentiment-Control. Table 6 reports the Control Accuracies, which represent the difference in accuracies between controlled and uncontrolled feedbacks, for both the baselines and the proposed models. These models take the desired sentiment for the feedback to portray as one of the input parameters: 0 for negative and 1 for positive. In uncontrolled settings, the parameter is not used and the control layer is disabled.

Table 6. Synthesized feedbacks’ sentiment analysis. Here, ‘USentiAcc’ and ‘CSentiAcc’ denote the sentiment classification accuracies for uncontrolled and controlled feedbacks respectively.

| Model | USentiAcc | CSentiAcc | Control Acc |
|-------------------|--------------|--------------|--------------|
| Baseline 1 | 52.34 | 63.10 | 10.76 |
| Baseline 2 | 54.72 | 67.06 | 12.34 |
| Baseline 3 | 48.25 | 57.32 | 9.07 |
| Baseline 4 | 52.48 | 71.57 | 19.09 |
| Proposed | 58.41 | 77.23 | 18.82 |

The sentiment class of the feedback is determined using FLAIR [1], SentimentR [57], DistilBERT [62], and RoBERTa [42], as detailed in Section 3.1. The model achieves a sentiment classification accuracy of 77.23% and a control accuracy of 18.82%. To calculate the sentiment accuracy, one

Table 7. Human evaluation of generated feedbacks where F_{UnCtrl} , $F_{PosCtrl}$ and $F_{NegCtrl}$ show uncontrolled, positively and negatively controlled feedbacks. Rel_{img} , Rel_{text} , $Rel_{Comment}$ and $Rel_{F_{UnCtrl}}$ are ‘relevant with’ input images, text, comments and uncontrolled feedback, respectively.

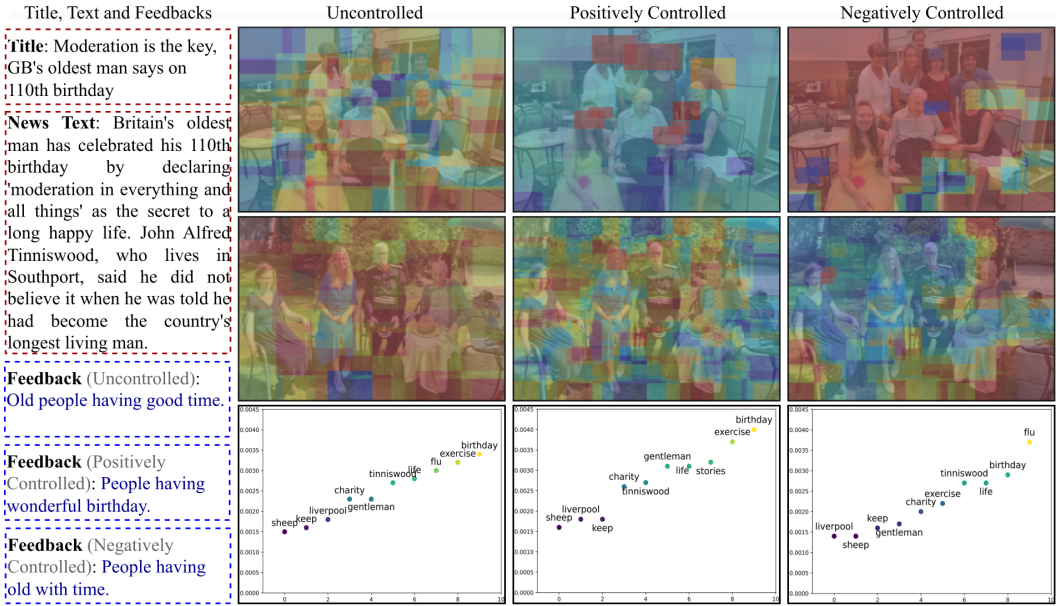
| | Rel_{img} | Rel_{text} | Comment | $Rel_{F_{UnCtrl}}$ |
|----------------|-------------|--------------|---------|--------------------|
| Comment | 70.85% | 72.93% | 100.00% | 78.27% |
| F_{UnCtrl} | 67.27% | 69.58% | 78.27% | 100.00% |
| $F_{PosCtrl}$ | 69.47% | 71.07% | 79.93% | 81.96% |
| $F_{NegCtrl}$ | 71.23% | 72.13% | 80.17% | 83.24% |

negative and one positive feedback is generated by passing the parameters—0 for negative and 1 for positive. The sentiment of the feedback is then calculated and compared to the ground truth sentiment labels.

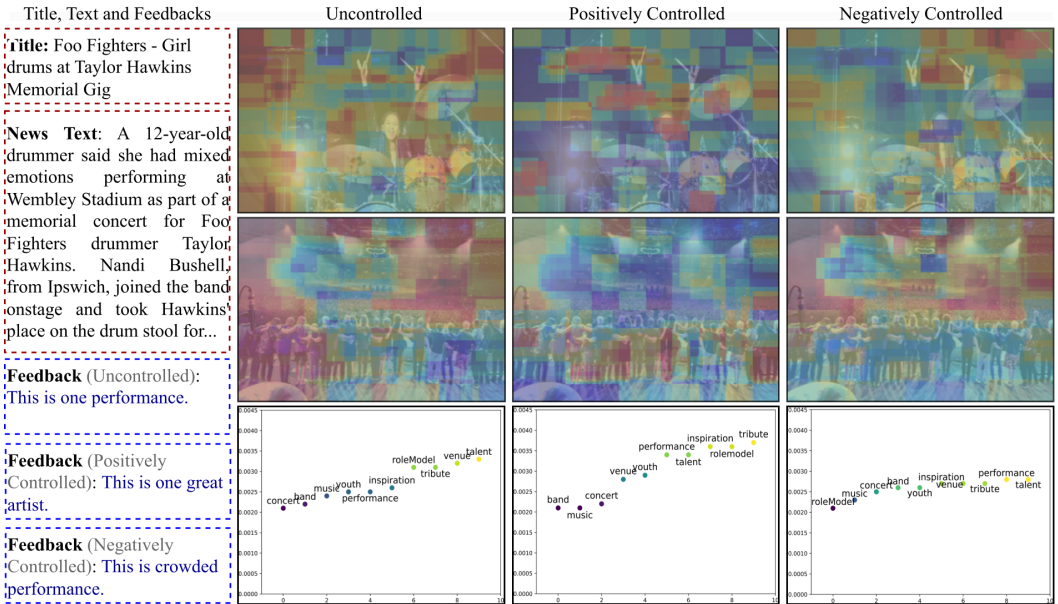
4.4.4 Compute Time Requirement. The total amount of compute time required for one epoch of model training on V100 GPU is as follows. Baseline 1 required 168 minutes, Baseline 2 was the most time-consuming at 233 minutes, Baseline 3 needed 144 minutes, and Baseline 4 was the fastest at 103 minutes. The Proposed System required 112 minutes to complete one epoch.

4.4.5 Interpretability and Visualization. The model-level and case-level interpretability analyses have been incorporated. Model-level interpretability is achieved by introducing perturbations to the feedback synthesis model via the control layer. The impact of these perturbations on the output feedback is detailed in Table 6 in terms of sentiment classification accuracies for uncontrolled and controlled (perturbed) scenarios. Fig. 3 shows sample results, highlighting the features being focused on during the generation of uncontrolled and controlled feedbacks. In image plots, red and blue represent the most and least contributing pixels, respectively whereas for text plots, yellow and blue indicate the most and least important textual features. In Fig. 3a, positive sentiments are indicated by smiling faces and a family setting, while negative sentiments are associated with the depiction of ageing, particularly in the older face. The expression of the girl on the left, a blend of smiling and discomfort, captures attention in both positive and negative contexts. The middle girl’s face, predominantly smiling, is highlighted in red for positive and blue for negative sentiments. Fig. 3b shows that dark areas contribute to negative sentiment, whereas faces are linked to positive sentiment. In negatively controlled settings, the crowd is focused; in positively controlled settings, the focus shifts to individual people. In Fig. 3c, positive sentiments downplay the importance of the gun, concentrating more on the number plate. In the uncontrolled setting, the focus is primarily on the words. For Fig. 3d, the facial features are highlighted red for positively controlled and blue for negatively controlled settings for the first image. The second image associates positive sentiment with light and text and negative sentiment with darkness.

4.4.6 Human Evaluation. : The sentiments of the generated feedbacks have been evaluated by 50 evaluators, comprising 25 males and 25 females, with an average age of 30 ± 2.73 years. They assessed the controlled and uncontrolled feedbacks for their valence and relevance with the inputs. A total of 50 randomly picked samples have been evaluated, and the averages of the evaluators’ scores have been reported. These scores for the relevance ratings for three types of feedback—uncontrolled, positive, and negative—against images and texts have been described in Table 7. On average, 72.68% and 78.14% evaluators reported that the sentiments of positively and negatively controlled feedbacks are more positive and more negative respectively than uncontrolled feedbacks’. The higher relevance scores for controlled feedbacks ($F_{PosCtrl}$ and $F_{NegCtrl}$) compared to uncontrolled ones (F_{UnCtrl}) confirm the control layer’s influences in feedback’s desired sentiment alignment.



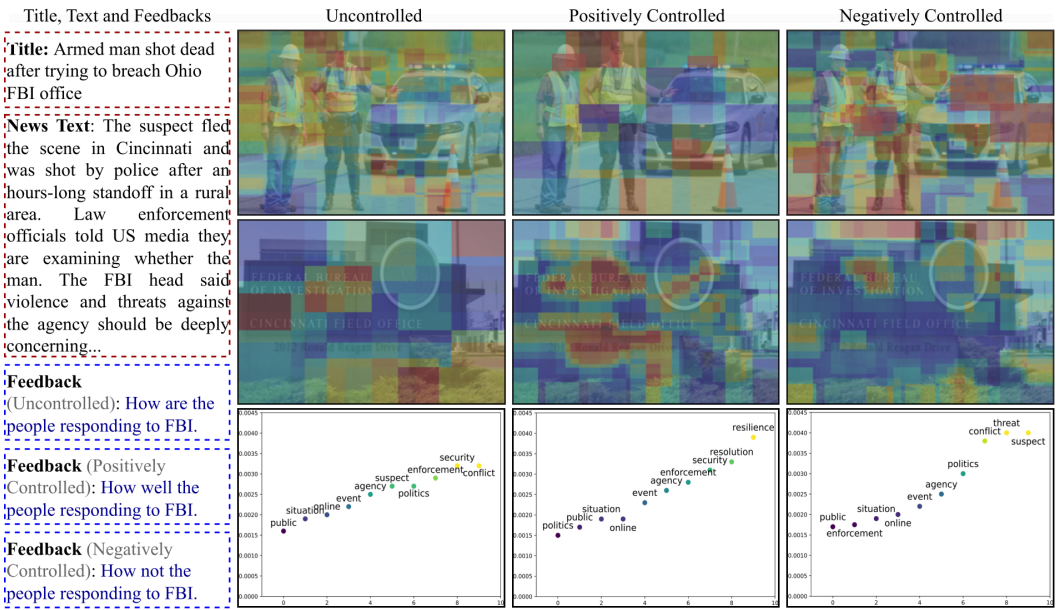
(a) Sample Result 1



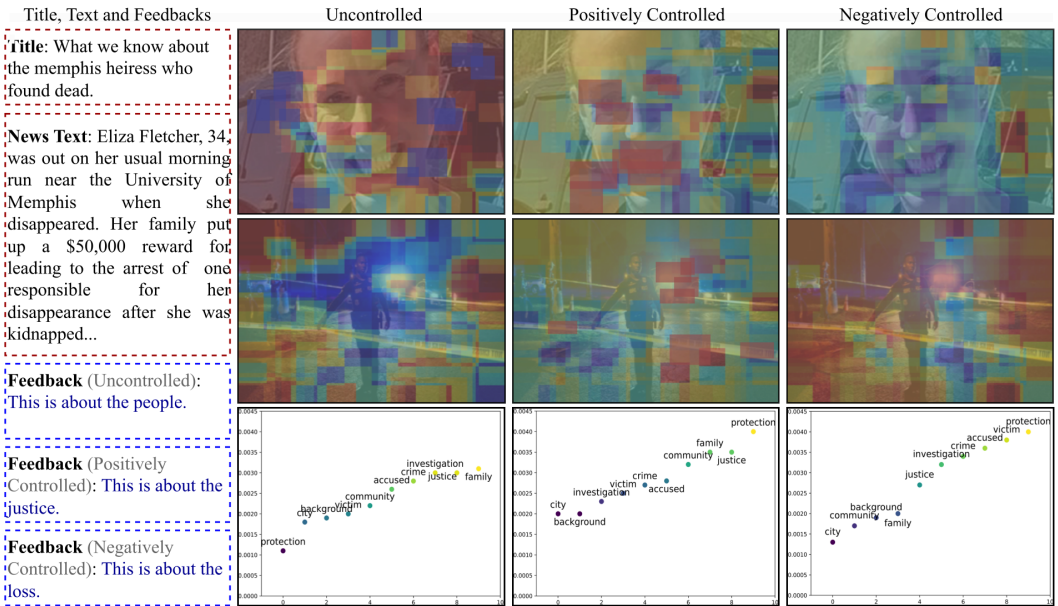
(b) Sample Result 2, continued on the next page.

4.4.7 Ablation Studies. Following ablation studies have been conducted to evaluate the impact of various parameters on the proposed system's performance.

1) Effect of Number of Control Layers and Value of Control-Parameter: The control layer has been used after the decoder and before the text generation phase to apply 'control' or constraints on the text generation. Here, it is crucial to decide a) the number of control layers and b) the suitable value



(c) Sample Result 3



(d) Sample Result 4

Fig. 3. Sample results along with interpretability plots. They depict the feedback generated by the proposed system using the news headline, text, and images (two out of multiple images shown) under the given sentiment-controllability constraint.

for the control parameter. Regarding the number of control layers, we experimented with 1, 2, 3, and 4 control layers. The best performance has been observed using the 1 control layer, which decreased slightly for 2 control layers, decreased further for 3 layers, and decreased significantly for 4 layers. Further, regarding the control parameter, we experimented with its values of 5%, 10%, 15%, and 20%. The results show that more control can be achieved with the increasing value of the control parameter; however, fewer neurons will get trained for the entire training data, causing a degradation in the result's quality. As depicted in Table 8, a control value of 10% results in better performance than the other values. Hence, 1 control layer with the control value of 10% has been used in the final implementation.

2) *Effect of Beam-size*: The beam-size is a search parameter that refers to the number of options the model keeps at each step of the prediction, controlling the breadth of the search for the best output sequence. It keeps only the top k predictions, where k is the beam size. A larger beam size allows the model to explore more possibilities, potentially improving output quality; however, it increases computational requirements and may also degrade the output because of repetitive text generation. We experimented with beam-size values of 2, 5, 10, 15, and 20. The corresponding sentiment classification accuracies and MRR values have been summarized in Table 8. As the beam-size value of 5 provides the best performance and computational complexity trade-off, it has been used in the final implementation.

Table 8. Ablation studies on control parameter, x and beam-size. The entries show sentiment classification accuracy/MRR.

| x / Beam-size | 2 | 5 | 10 | 15 | 20 |
|-----------------|-----------------|------------------------|-----------------|-----------------|-----------------|
| 5 | 66.92% / 0.3505 | 76.89% / 0.3605 | 52.83% / 0.3641 | 54.51% / 0.3214 | 50.40% / 0.3491 |
| 10 | 71.42% / 0.3483 | 77.23% / 0.3789 | 64.81% / 0.3390 | 50.48% / 0.3393 | 47.36% / 0.3503 |
| 15 | 52.82% / 0.3429 | 69.71% / 0.3548 | 54.99% / 0.3312 | 60.40% / 0.3523 | 45.24% / 0.3449 |
| 20 | 64.57% / 0.3354 | 75.12% / 0.3389 | 57.76% / 0.3355 | 49.63% / 0.3409 | 41.46% / 0.3295 |

3) *Effect of Division Factor for KAAP technique*: The suitable values of the division factors k_{img} and k_{txt} used in Section 3.3.7 have been decided experimentally using the dice coefficient [16]. It measures the similarity of two data samples; the value of 1 denotes that the two compared data samples are completely similar, whereas a value of 0 denotes their complete dis-similarity. For each modality, we computed the KAAP values at $k \in \{2, 3, \dots, 30\}$ and analyzed the dice coefficients for two adjacent k values. For image & text, the dice coefficient values converge to 1 at k values of 5 and 20 respectively. Hence, the same have been used by the proposed system.

5 DISCUSSION AND CONCLUSION

In this section, we discuss the progression, draw conclusions from critical outcomes of our research, explore the limitations encountered, and outline the future directions for enhancing the controllability and effectiveness of feedback synthesis systems.

Advancements from Uncontrolled to Controllable Feedback Synthesis: The proposed controllable feedback synthesis system builds on our pioneering work on uncontrolled feedback synthesis [35], which utilized a basic dataset collected from Twitter lacking detailed comment metadata. The current system enhances both the control and interpretability of feedback. It addresses the challenge of comment relevance in the CMFeed dataset by adopting Facebook's relevance criteria. Despite slightly lower 'R@k' values due to more comments per sample (10.5 compared to 8.5), the improved MRR value (0.3789 versus 0.3042) highlights the effectiveness of the implemented similarity module. The

proposed system, trained on human comments and image-text inputs under sentiment constraints, generates human-like feedback with appropriate sentiments, evidenced by metrics in Tables 4 and 5. The control layer facilitates the generation of feedback with desired sentiments, utilizing different non-keywords and varying keywords, especially at higher control parameter values.

Ethical Considerations, Data Privacy, and Potential Misuse: All data collection adheres to ethical guidelines with rigorous processes to ensure privacy and consent. Publicly available data has been manually scraped in accordance with Facebook’s ethical guidelines, which prohibit automatic scraping [18]. Ethical protocols for scraping data from Facebook were strictly adhered to [6]. Data from public news channels and Facebook posts is collected manually to comply with platform policies, and human-generated comments are included without identifying information. Furthermore, while any technology can be misused, we have proactively designed our feedback synthesis system with an integral interpretability module. This feature is crucial for explaining decision-making within the system and for detecting and preventing misuse, such as creating misleading content. Our goal is to ensure responsible and ethical use, enhancing positive impact while minimizing risks. By developing robust and transparent systems, we aim to foster trust and encourage responsible technology use in line with our ethical commitments.

Dataset Generalizability and Diversity: With 3.07 billion of the total 5 billion social media users, the extensive user base of Facebook, reflective of broader social media engagement patterns, ensures that the insights gained are applicable across various platforms, reducing bias and strengthening the generalizability of our findings. Additionally, the geographic and political diversity of these selected news sources, which range from local (NY Daily News) to international (BBC News) coverage and span the political spectrum from left (NY Daily News) to right (Fox News), ensures a balanced representation of global and political viewpoints in our dataset. This approach not only mitigates regional and ideological biases but also enriches the dataset with a wide array of perspectives, further solidifying the robustness and applicability of our research. Other large-scale news handles like NDTV, The Hindu, Xinhua, and SCMP were considered but not selected, as their content is often in regional languages such as Hindi or Chinese, which could limit the accessibility and relevance of the data.

Dataset Selection and Integration Considerations: We found a Reddit dataset containing human comments [54], but opted not to include it in the considered datasets (Table 1) due to several issues. The source was deemed unreliable as it included a torrent download link and lacked associated scholarly publications. Moreover, the associated metadata was not comprehensive and did not appear to adhere to ethical protocols. These factors, along with the dataset’s unstructured and varied user-generated content and Reddit’s open forum format, which complicates data verification and includes potentially unreliable content, led to its exclusion. Furthermore, the informal nature of Reddit discussions does not align with the structured sentiment analysis required for news discourse. Additionally, we chose not to merge data from platforms such as Reddit and Twitter with Facebook due to the lack of comprehensive metadata, clear ethical guidelines, and control mechanisms—such as who can comment and whether users’ anonymity is maintained—on these platforms other than Facebook. These factors are critical for our analysis. Our focus on Facebook alone was crucial to ensure consistency in data quality and format.

Limitations: The efficacy of the CMFeed dataset is subject to several limitations, closely linked to data diversity and quality. Collection biases from specific platforms or demographics may impact generalizability. Technological constraints also limit the deployment of our system; substantial computational resources are required, which may not be readily available in all scenarios. Furthermore,

adding modalities such as audio and physiological data may introduce privacy and ethical challenges. There is a risk of technology misuse in manipulating user sentiments and potential biases in sentiment analysis, which could result in over-reliance on automation, reduced human empathy, and unethical applications of feedback synthesis. These limitations highlight the need for cautious and responsible use of AI technologies, ensuring that ethical standards are rigorously maintained and biases are systematically addressed.

Future Plans: We aim to refine our feedback generation by integrating discrete emotion classes, enhancing the emotional depth of the responses. Additionally, we plan to incorporate more modalities, including audio and physiological signals, to enrich the multimodal input and make the system more empathetic. We will also develop control over other feedback aspects, such as emotion intensity and duration, to tailor responses more precisely. Finally, we will test these advancements in real-life applications, such as education, healthcare, marketing and customer service, to assess their practical effectiveness and ensure they adhere to ethical standards.

ACKNOWLEDGEMENTS

This work was supported by the University of Oulu and the Research Council of Finland Profi 5 HiDyn fund (grant 2463011132). The authors acknowledge the CSC-IT Center for Science, Finland, for providing computational resources.

REFERENCES

- [1] Alan Akbik, Tanja Bergmann, et al. 2019. FLAIR: An Easy-to-Use Framework For State-Of-The-Art NLP. In 2019 Conf. of North American Chapter of Association for Comp. linguistics (NAACL). 54–59.
- [2] Peter Anderson, Basura Fernando, et al. 2016. SPICE: Semantic Propositional Image Caption Evaluation. In The European Conference on Computer Vision (ECCV). 382–398.
- [3] Stanislaw Antol, Aishwarya Agrawal, et al. 2015. VQA: Visual Question Answering. In The 19th IEEE/CVF International Conference on Computer Vision (ICCV). 2425–2433.
- [4] Steven Bird, Ewan Klein, and Edward Loper. [n. d.]. NLTK Documentation. Accessed 05 Oct 2024.
- [5] Paulo Blikstein and Marcelo Worsley. 2016. Multimodal Learning analytics and Education Data Mining: Using Computational Technologies to Measure Complex Learning Tasks. Journal of Learning Analytics 3, 2 (2016), 220–238.
- [6] The Web Scraping Blog. 2024. How to Scrape Facebook Ethically in 2024. <https://webscraping.blog/how-to-scrape-facebook> Accessed 05 Oct 2024.
- [7] Carlos Busso et al. 2008. IEMOCAP: Interactive Emotional Dyadic Motion Capture Database. Language Resources and Evaluation 42 (2008), 335–359.
- [8] Paola Cascante-Bonilla, Hui Wu, et al. 2022. SimVQA: Exploring Simulated Environments for Visual Question Answering. In IEEE/CVF Conf. on Computer Vision and Pattern Recognition (CVPR). 5056–5066.
- [9] Pew Research Center. 2024. Social Media Fact Sheet. <https://pewresearch.org/internet/fact-sheet/social-media/> Accessed 05 Oct 2024.
- [10] Feilong Chen, Xiuyi Chen, et al. 2022. Improving Cross-Modal Understanding In Visual Dialog Via Contrastive Learning. In IEEE International Conference on Acoustics, Speech and Signal Processing (ICASSP). 7937–7941.
- [11] Feng Chen, Jiayuan Xie, et al. 2023. Graph Convolutional Net For Difficulty-Controllable Visual Ques. Generation. World Wide web (www) (2023), 1–23.
- [12] Jingqiang Chen and Hai Zhuge. 2018. Abstractive Text-Image Summarization Using Multimodal Attention Hierarchical RNN. In The Conference on Empirical Methods in Natural Language Processing (EMNLP). 4046–4056.
- [13] Nick Craswell. 2009. Mean Reciprocal Rank. Encyclopedia of Database Systems 1703 (2009).
- [14] Abhishek Das, Satwik Kottur, et al. 2017. Learning Cooperative Visual Dialog Agents With Deep Reinforcement Learning. In The 21th IEEE/CVF International Conference on Computer Vision (ICCV). 2951–2960.
- [15] Abhishek Das, Satwik Kottur, Khushi Gupta, Avi Singh, Deshraj Yadav, José M.F. Moura, Devi Parikh, and Dhruv Batra. 2017. Visual Dialog. In Proceedings of the IEEE/CVF Conference on Computer Vision and Pattern Recognition (CVPR).
- [16] Ruoxi Deng, Chunhua Shen, et al. 2018. Learning To Predict Crisp Boundaries. In The European Conference on Computer Vision (ECCV). 562–578.

- [17] Facebook. 2024. [Data Scraping and What Can You do to Protect Your Information on Facebook](https://khoros.com/resources/social-media-demographics-guide). <https://khoros.com/resources/social-media-demographics-guide> Accessed 05 Oct 2024.
- [18] Facebook. 2024. [Social Media Demographics Guide](https://www.facebook.com/help/463983701520800). <https://www.facebook.com/help/463983701520800> Accessed 05 Oct 2024.
- [19] Sebastian Farquhar, Jannik Kossen, Lorenz Kuhn, and Yarin Gal. 2024. Detecting Hallucinations in Large Language Models Using Semantic Entropy. *Nature* 630, 8017 (2024), 625–630.
- [20] Mauajama Firdaus, Hardik Chauhan, et al. 2020. EmoSen: Generating Sentiment And Emotion Controlled Responses In A Multimodal Dialogue System. *IEEE Transactions on Affective Computing* 13, 3 (2020), 1555–1566.
- [21] Mauajama Firdaus, Umang Jain, et al. 2021. SEPRG: Sentiment Aware Emotion Controlled Personalized Response Generation. In *Proceedings of the 14th International Conference on Natural Language Generation (INLG)*. 353–363.
- [22] Fabio R Gallo, Gerardo I Simari, et al. 2020. Predicting User Reactions to Twitter Feed Content based on Personality Type and Social Cues. *Future Generation Computer Systems* 110 (2020), 918–930.
- [23] Yash Goyal, Tejas Khot, Douglas Summers-Stay, Dhruv Batra, and Devi Parikh. 2017. Making the V in VQA Matter: Elevating the Role of Image Understanding in Visual Question Answering. In *Proceedings of the IEEE Conference on Computer Vision and Pattern Recognition (CVPR)*. 6904–6913.
- [24] Zhicheng Guo, Jiaxuan Zhao, et al. 2021. A Universal Quaternion Hypergraph For Multimodal VQA. *IEEE Transactions on Multimedia* (2021).
- [25] Jiaxiong Hu, Yun Huang, et al. 2022. The Acoustically Emotion-Aware Conversational Agent With Speech Emotion And Empathetic Responses. *IEEE Transactions on Affective Computing* 14, 1 (2022), 17–30.
- [26] Chenyang Huang, Osmar R Zaiane, et al. 2018. Automatic Dialogue Generation With Expressed Emotions. In *The Conference of North American Chapter of the Association for Computational Linguistics (NAACL)*. 49–54.
- [27] Lei Huang, Weijiang Yu, Weitao Ma, Weihong Zhong, Zhangyin Feng, Haotian Wang, Qianglong Chen, Weihua Peng, Xiaocheng Feng, Bing Qin, et al. 2023. A Survey on Hallucination in Large Language Models: Principles, Taxonomy, Challenges, and Open Questions. *arXiv preprint arXiv:2311.05232* (2023). Accessed 05 Oct 2024.
- [28] Md Farhan Ishmam, Md Sakib Hossain Shovon, Muhammad Firoyz Mridha, and Nilanjan Dey. 2024. From Image to Language: A Critical Analysis of Visual Question Answering (VQA) Approaches, Challenges, And Opportunities. *Information Fusion* (2024), 102270.
- [29] Xiaozhe Jiang et al. 2020. DualVD: An Adaptive Dual Encoding Model for Deep Visual Understanding in Visual Dialogue. In *The 34th AAAI Conference on Artificial Intelligence (AAAI)*, Vol. 34. 11125–11132.
- [30] Zan-Xia Jin, Heran Wu, et al. 2021. RUArt: A Novel Text-Centered Text-Based Visual Question Answering. *IEEE Transactions on Multimedia* (2021).
- [31] Gi-Cheon Kang, Sungdong Kim, et al. 2023. The Dialog Must Go On: Improving Visual Dialog via Generative Self-Training. In *IEEE/CVF Conference on Computer Vision and Pattern Recognition (CVPR)*. 6746–6756.
- [32] Gi-Cheon Kang, Jaeseo Lim, et al. 2019. Dual Attention Networks for Visual Reference Resolution in Visual Dialog. In *The Conference on Empirical Methods in Natural Language Processing (EMNLP)*. 2024–2033.
- [33] Xiang Kong, Bohan Li, et al. 2019. An Adversarial Approach To Sentiment-Controlled Neural Dialogue Generation. *arXiv preprint arXiv:1901.07129* (2019). Accessed 05 Oct 2024.
- [34] Satwik Kottur, José MF Moura, Devi Parikh, Dhruv Batra, and Marcus Rohrbach. 2019. CLEVR-Dialog: A Diagnostic Dataset for Multi-Round Reasoning in Visual Dialog. In *Proceedings of Annual Conference of the North American Chapter of the Association for Computational Linguistics (NAACL-HLT)*. 582–595.
- [35] Puneet Kumar, Gaurav Bhatt, Omkar Ingle, Daksh Goyal, and Balasubramanian Raman. 2023. Affective Feedback Synthesis Towards Multimodal Text and Image Data. *ACM Transactions on Multimedia Computing, Communications and Applications* 19, 6 (2023), 1–23.
- [36] Puneet Kumar, Sarthak Malik, Balasubramanian Raman, and Xiaobai Li. 2022. VISTANet: Visual Spoken Textual Additive Net for Interpretable Multimodal Emotion Recognition. *arXiv preprint arXiv:2208.11450* (2022). Accessed 05 Oct 2024.
- [37] Alon Lavie and Michael J Denkowski. 2009. The METEOR Metric for Automatic Evaluation of Machine Translation. *Springer Machine Translation Journal* 23, 2-3 (2009), 105–115.
- [38] Jens Lehmann et al. 2023. Language Models As Controlled Natural Language Semantic Parsers For Knowledge Graph Question Answering. In *European Conference on Artificial Intelligence (ECAI)*, Vol. 372. IOS Press, 1348–1356.
- [39] Chin-Yew Lin. 2004. ROUGE: A Package for Automatic Evaluation of Summaries. In *Text Summarization Branches Out, Association for Computational Linguistics (ACL)*. 74–81.
- [40] An-An Liu, Chenxi Huang, et al. 2023. Counterfactual Visual Dialog: Robust Commonsense Knowledge Learning From Unbiased Training. *IEEE Transactions on Multimedia* (2023).
- [41] An-An Liu, Guokai Zhang, et al. 2022. Closed-Loop Reasoning With Graph-Aware Dense Interaction For Visual Dialog. *Multimedia Systems* 28, 5 (2022), 1823–1832.

- [42] Yinhan Liu, Myle Ott, et al. 2019. RoBERTa: A Robustly Optimized BERT Pretraining Approach. [arXiv preprint arXiv:1907.11692](https://arxiv.org/abs/1907.11692) (2019). Accessed 05 Oct 2024.
- [43] Mariana Rodrigues Makiuchi, Kuniaki Uto, et al. 2021. Multimodal Emotion Recognition with High-level Speech and Text Features. In [IEEE Automatic Speech Recognition and Understanding Workshop \(ASRU\)](#).
- [44] Kenneth Marino, Mohammad Rastegari, Ali Farhadi, and Roozbeh Mottaghi. 2019. OK-VQA: A Visual Question Answering Benchmark Requiring External Knowledge. In [Proceedings of the IEEE/CVF Conference on Computer Vision and Pattern Recognition \(CVPR\)](#). 3195–3204.
- [45] Minesh Mathew, Ruben Tito, Dimosthenis Karatzas, R Manmatha, and CV Jawahar. 2020. Document visual question answering challenge 2020. In [IEEE/CVF Conf. on Computer Vision and Pattern Recognition \(CVPR\) Workshop](#).
- [46] Meta. [n. d.]. [Facebook Terms and Conditions](#). Accessed 05 Oct 2024.
- [47] Michal Muszynski et al. 2019. Recognizing Induced Emotions of Movie Audiences from Multimodal Information. [IEEE Transactions on Affective Computing](#) 12, 1 (2019), 36–52.
- [48] Teng Niu, Shiai Zhu, Lei Pang, and Abdulmotaleb El Saddik. 2016. Sentiment analysis on multi-view social data. In [22nd International Conference on MultiMedia Modeling \(MMM\)](#). Springer, 15–27.
- [49] OpenAI. 2019. [GPT2](#). Accessed 05 Oct 2024.
- [50] Lucas Ou-Yang. [n. d.]. [Newspaper3k Documentation](#). Accessed 05 Oct 2024.
- [51] Mathieu Page Fortin and Brahim Chaib-draa. 2019. Multimodal Multitask Emotion Recognition Using Images, Texts and Tags. In [The ACM International Conference on Multimedia Retrieval \(ICMR\)](#). 3–10.
- [52] Kishore Papineni, Salim Roukos, et al. 2002. BLEU: A Method for Automatic Evaluation of Machine Translation. In [The 40th Annual Meeting on Association for Computational Linguistics \(ACL\)](#). 311–318.
- [53] Alec Radford, Karthik Narasimhan, et al. 2018. Improving Language Understanding by Generative Pre-training. [OpenAI](#) (2018).
- [54] Reddit. 2015. [Reddit Dataset](#). www.reddit.com/r/datasets/comments/3bxl7g/i_have_every_publicly_available_reddit_comment/ Accessed 05 Oct 2024.
- [55] Nils Reimers and Iryna Gurevych. 2019. Sentence-BERT: Sentence Embeddings using Siamese BERT-Networks. In [Conference on Empirical Methods in Natural Language Processing and International Joint Conference on Natural Language Processing \(EMNLP-IJCNLP\)](#). 3982–3992.
- [56] Shaoqing Ren, Kaiming He, et al. 2015. Faster R-CNN: Towards Real-Time Object Detection with Region Proposal Networks. [Advances in Neural Information Processing Systems \(NeurIPS\)](#) 28 (2015), 91–99.
- [57] Tyler Rinker. 2017. [SentimentR Package for R Language](#). Accessed 05 Oct 2024.
- [58] Adrian Rosebrock. 2016. Intersection Over Union (IoU) for Object Detection. <https://www.pyimagesearch.com/2016/11/07/intersection-over-union-iou-for-object-detection>. [PyImageSearch.com](#) (2016). Accessed 05 Oct 2024.
- [59] Per Runeson, Magnus Alexandersson, and Oskar Nyholm. 2007. Detection of Duplicate Defect Reports using Natural Language Processing. In [International Conference on Software Engineering](#). 499–510.
- [60] Tulika Saha, Aditya Patra, Sriparna Saha, and Pushpak Bhattacharyya. 2020. Towards Emotion-Aided Multi-Modal Dialogue Act Classification. In [Proceedings of the 58th Annual Meeting of the Association for Computational Linguistics \(ACL\)](#). 4361–4372.
- [61] Tulika Saha, Sriparna Saha, et al. 2022. Towards Sentiment-Aware Multi-Modal Dialogue Policy Learning. [Cognitive Computation](#) (2022), 1–15.
- [62] Victor Sanh, Lysandre Debut, et al. 2019. DistilBERT, A Distilled Version of BERT: Smaller, Faster, Cheaper and Lighter. [arXiv preprint arXiv:1910.01108](https://arxiv.org/abs/1910.01108) (2019). Accessed 05 Oct 2024.
- [63] Lifeng Shang, Zhengdong Lu, and Hang Li. 2015. Neural Responding Machine for Short-Text Conversation. In [Proceedings of the 53rd Annual Meeting of the Association for Computational Linguistics and the 7th International Joint Conference on Natural Language Processing \(ACL-IJCNN\)](#). 1577–1586.
- [64] Xindi Shang, Zehuan Yuan, et al. 2021. Multimodal Video Summarization Via Time-Aware Transformers. In [29th ACM International Conference on Multimedia \(MM\)](#). 1756–1765.
- [65] LS Shapley. 1953. A Value for n-Person Games, Contributions to the Theory of Games II.
- [66] Weiyan Shi and Zhou Yu. 2018. Sentiment Adaptive End-to-End Dialog Systems. In [56th Annual Meeting of the Association for Computational Linguistics \(ACL\)](#). 1509–1519.
- [67] Sprout Social. 2024. [New Social Media Demographics](#). sproutsocial.com/insights/new-social-media-demographics/ Accessed 05 Oct 2024.
- [68] Brad Solomon. [n. d.]. [Demoji Documentation](#). Accessed 05 Oct 2024.
- [69] Ashish Vaswani, Noam Shazeer, et al. 2017. Attention Is All You Need. In [Advances in Neural Information Processing Systems \(NeurIPS\)](#). 5998–6008.
- [70] Ramakrishna Vedantam, C Lawrence Zitnick, et al. 2015. CIDEr: Consensus-based Image Description Evaluation. In [IEEE/CVF Conference on Computer Vision and Pattern Recognition \(CVPR\)](#). 4566–4575.

- [71] Ke Wang and Xiaojun Wan. 2018. SentiGAN: Generating Sentimental Texts Via Mixture Adversarial Networks. In International Joint Conference on Artificial Intelligence (IJCAI). 4446–4452.
- [72] Peng Wang, Qi Wu, et al. 2017. FVQA: Fact-Based Visual Question Answering. IEEE Transactions on Pattern Analysis and Machine Intelligence 40, 10 (2017), 2413–2427.
- [73] Zihao Wang, Junli Wang, et al. 2022. Unified Multimodal Model With Unlikelihood Training For Visual Dialog. In The 30th ACM International Conference on Multimedia (MM). 4625–4634.
- [74] Bingbing Wen, Zhengyuan Yang, Jianfeng Wang, Zhe Gan, Bill Howe, and Lijuan Wang. 2023. InfoVisDial: An Informative Visual Dialogue Dataset by Bridging Large Multimodal and Language Models. arXiv preprint arXiv:2312.13503 (2023).
- [75] Wikipedia. 2024. List of Social Platforms with at Least 100 Million Active Users. https://en.wikipedia.org/wiki/List_of_social_platforms_with_at_least_100_million_active_users Accessed 05 Oct 2024.
- [76] Jinneng Wu, Tingting Mu, et al. 2023. Memory-Aware Attentive Control For Community Question Answering With Knowledge-Based Dual Refinement. IEEE Transactions on Systems, Man, and Cybernetics: Systems (2023).
- [77] Shih-Lun Wu, Chris Donahue, Shinji Watanabe, and Nicholas J Bryan. 2024. Music ControlNet: Multiple Time-Varying Controls for Music Generation. IEEE/ACM Transactions on Audio, Speech, and Language Processing 32 (2024), 2692–2703.
- [78] Yu Wu, Furu Wei, et al. 2019. Response Generation by Context Aware Prototype Editing. In The 33rd AAAI Conference on Artificial Intelligence (AAAI), Vol. 33. 7281–7288.
- [79] Jiehang Xie, Xuanbai Chen, et al. 2022. Multimodal-Based And Aesthetic-Guided Narrative Video Summarization. IEEE Transactions on Multimedia (2022).
- [80] Dejing Xu, Zhou Zhao, Jun Xiao, Fei Wu, Hanwang Zhang, Xiangnan He, and Yueting Zhuang. 2017. Video Question Answering via Gradually Refined Attention over Appearance and Motion. In ACM Multimedia (MM).
- [81] Xinnuo Xu, Ondřej Dušek, et al. 2018. Better Conversations By Modeling, Filtering, And Optimizing For Coherence And Diversity. arXiv preprint arXiv:1809.06873 (2018). Accessed 05 Oct 2024.
- [82] Yukang Yang, Dongnan Gui, Yuhui Yuan, Weicong Liang, Haisong Ding, Han Hu, and Kai Chen. 2024. GlyphControl: Glyph Conditional Control for Visual Text Generation. Advances in Neural Information Processing Systems (NeurIPS) 36 (2024).
- [83] Licheng Yu, Eunbyung Park, Alexander C Berg, and Tamara L Berg. 2015. Visual Madlibs: Fill in the Blank Description Generation and Question Answering. In Proceedings of the IEEE/CVF International Conference on Computer Vision (CVPR). 2461–2469.
- [84] Rowan Zellers et al. 2020. VMSMO: Learning to Generate Multimodal Summary for Video-based News Articles. In The Conference on Empirical Methods in Natural Language Processing (EMNLP). 9360–9369.
- [85] Bin Zhao, Maoguo Gong, and Xuelong Li. 2021. Audio-Visual Video Summarization. IEEE Transactions on Neural Networks and Learning Systems (2021).
- [86] Tiancheng Zhao et al. 2017. Learning Discourse-Level Diversity For Neural Dialog Models Using Conditional Variational Autoencoders. In The 55th Annual Meeting of Association for Comp. Linguistics (ACL). 654–664.
- [87] Peixiang Zhong et al. 2019. An Affect-Rich Neural Conversational Model With Biased Attention And Weighted Cross-Entropy Loss. In AAAI Conference on Artificial Intelligence (AAAI), Vol. 33. 7492–7500.
- [88] Hao Zhou, Minlie Huang, Tianyang Zhang, Xiaoyan Zhu, and Bing Liu. 2018. Emotional Chatting Machine: Emotional Conversation Generation with Internal and External Memory. In Proceedings of the AAAI Conference on Artificial Intelligence (AAAI), Vol. 32.
- [89] Junnan Zhu, Haoran Li, et al. 2018. MSMO: Multimodal Summarization With Multimodal Output. In The Conference on Empirical Methods in Natural Language Processing (EMNLP). 4154–4164.
- [90] Junnan Zhu, Yu Zhou, et al. 2020. Multimodal Summarization With Guidance of Multimodal Reference. In The 34th AAAI Conference on Artificial Intelligence (AAAI), Vol. 34. 9749–9756.
- [91] Yubo Zhu, Wentian Zhao, et al. 2023. Topic-Aware Video Summarization Using Multimodal Transformer. Pattern Recognition 140 (2023), 109578.